Metallic photonic crystals with strong broadband absorption at optical frequencies over wide angular range

Georgios Veronis, Robert W. Dutton, and Shanhui Fan[a)]
Department of Electrical Engineering, Stanford University, Stanford, California 94305

We show theoretically that a finite two-dimensional square lattice of metallic cylinders in air can be designed to have almost 100% absorptance over a wide optical wavelength range and for a wide range of incidence angles. The broadband and wide-angle strong absorption is attributed to the presence of a large number of flat bands interacting with air bands and the greatly improved impedance matching between metallic photonic crystals and air. The frequency band of intense absorption is in the visible, ultraviolet, or near infrared, depending on the metallic material. © *2005 American Institute of Physics*. [DOI: 10.1063/1.1889248]

I. INTRODUCTION

Developing materials and structures that have unusual absorption characteristics in the optical wavelength range is important for applications such as photovoltaics,[1,2] control of thermal radiation,[3,4] and photodetectors.[5,6]

Photonic crystals consisting of metallic materials exhibit a number of interesting properties at optical frequencies, if properly designed. In particular, one-dimensional photonic crystals composed of a stack of alternating layers of metallic and dielectric materials can be designed to be transparent over a tunable range of optical frequencies.[7,8] These structures can also be designed to enhance reflection[9] or absorption.[10] In addition, three-dimensional metallic photonic crystals can exhibit absorption suppression in the photonic band gap and strong absorption enhancement at the photonic band edge.[3,4] The enhancement is attributed to the slower group velocity of light at the band edge.

There have been several previous studies on the absorption properties of metallic photonic crystals.[10–17] However, they were limited to small angles of incidence and did not investigate the conditions for creating strong wide-angle absorption. In this article, we show that photonic crystals consisting of metallic cylinders can be designed to have almost 100% absorptance over a wide wavelength range and for a wide range of incidence angles.

II. MODEL DESCRIPTION

We calculate the transmittance, reflectance and absorptance for plane waves normally or obliquely incident on a slab of metallic photonic crystal with infinite extent in the transverse directions [Fig. 1(a)] using a finite-difference frequency-domain (FDFD) method.[18–21] A single period of the slab of photonic crystal is placed in the middle of the computational domain with its top and bottom surfaces normal to the z direction [Fig. 1(b)]. Plane waves are generated by exciting a planar current source normal to the z direction with a phase factor $\exp(i\mathbf{k}_0 \cdot \mathbf{r})$, where $\mathbf{k}_0 = \omega(\epsilon_0\mu_0)^{1/2}\hat{\mathbf{u}}$, and $\hat{\mathbf{u}}$

defines the direction of the incident wave. Perfectly matched layer (PML) absorbing boundary conditions[22] are used at the top and bottom boundaries, while on all other boundaries we use the following condition for the electric field:

$$\mathbf{E}(\mathbf{r} + \mathbf{a}) = \exp(i\mathbf{k}_0 \cdot \mathbf{a})\mathbf{E}(\mathbf{r}),$$

where $\mathbf{a}$ is the lattice vector. This condition takes into account the periodicity of the structure. Maxwell's equations are discretized in the computational domain and solved using FDFD. Fields are monitored at detector points above and below the crystal. The incident wave fields are calculated at the detector points by performing a simulation without the crystal.[23] The transmission and reflection coefficients are then calculated, while the absorption coefficient is obtained by energy conservation.

To perform band structure calculations with FDFD, we use a single unit cell of the crystal as the computational domain and apply Bloch's condition at all boundaries

$$\mathbf{E}(\mathbf{r} + \mathbf{a}) = \exp(i\mathbf{k} \cdot \mathbf{a})\mathbf{E}(\mathbf{r}),$$

where $\mathbf{k}$ is the wave vector. We excite a point source and the resulting spectrum at a detector point is composed of a discrete set of peaks, where each peak corresponds to an eigen-
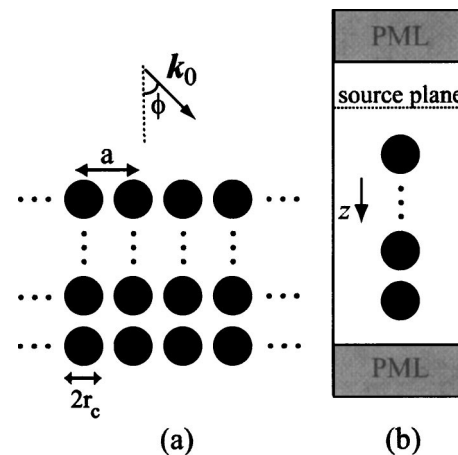

FIG. 1. (a) Schematic of the simulated structure. (b) Schematic of the computational domain used in the FDFD method.

[a)]Author to whom correspondence should be addressed; electronic mail: shanhui@stanford.edu
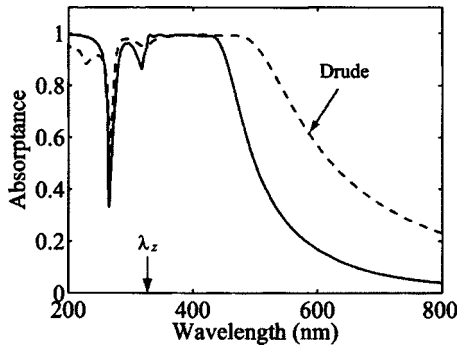
97, 093104-1

FIG. 2. Absorption spectrum of a finite two-dimensional square lattice of silver cylinders in air consisting of 45 layers in the z direction for normal incidence and H polarization. The lattice parameters are $a = 130$ nm, $r_c = 15$ nm. The dashed line shows the absorption spectrum calculated using the Drude model with parameters $\omega_p = 6.9$ eV, $\gamma = 0.48$ eV.

FIG. 3. (a)–(d) Absorption spectrum of the structure of Fig. 2 for incidence angles $\phi = 20°$, $40°$, $60°$, and $70°$, respectively. The dashed lines mark the wavelength range 328 nm $\leq \lambda \leq$ 437 nm.

frequency. The method is similar to the band structure calculation using FDTD.[23] Alternatively, band structure calculations with FDFD can be performed using an eigenvalue approach.[20,21]

FDFD has several inherent advantages for transmission and band structure calculations of metallic photonic crystals. It is not limited to specific geometrical structures such as cylinders or spheres. In contrast to FDTD, it enables modeling of arbitrary frequency-dependent dielectric constants. Finally, transmission calculations are numerically stable for any slab thickness.

III. RESULTS

Using FDFD, we calculate the absorptance of a finite two-dimensional square lattice of silver cylinders in air, consisting of 45 layers in the z direction. We use experimental data for the frequency-dependent dielectric constant of silver.[24] The structure is characterized by the lattice constant a and the cylinder radius r_c [Fig. 1(a)]. In Fig. 2, we show the absorptance for normal incidence and H polarization. The lattice parameters are $a = 130$ nm, $r_c = 15$ nm. We also show $\lambda_z \simeq 328$ nm corresponding to the first zero crossing of the real part of the dielectric constant of silver[24] ϵ_{silver}. We observe a wide frequency band 328 nm $\leq \lambda \leq$ 437 nm in which absorption exceeds 99%.

For metallic structures at optical frequencies, most studies invoke the Drude model to characterize the frequency dependence of the dielectric function[14–17,25–29]

$$\epsilon(\omega) = 1 - \frac{\omega_p^2}{\omega(\omega - i\gamma)},$$

where ω_p, γ are frequency-independent parameters. In Fig. 2, we also show the absorptance of the structure calculated with the Drude model. The two parameters of the model ω_p and γ were chosen so that the error in the dielectric constant with respect to the experimental data is minimized in the frequency band of intense absorption 328 nm $\leq \lambda \leq$ 437 nm. We observe that the use of the Drude model results in substantial error. In particular, the frequency range of intense absorption is substantially overestimated. The Drude model is therefore
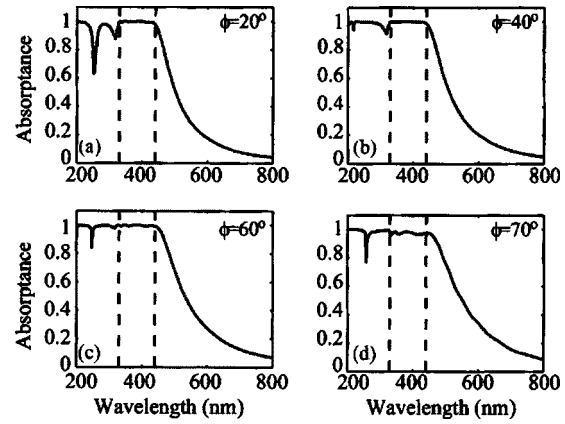
inadequate for accurate calculation of the absorption spectrum.[30]

We also calculate the absorptance for obliquely incident waves. In Figs. 3(a)–3(d), we show the absorptance for different angles of incidence. The structure is the same as in Fig. 2. We observe that for a wide angular range $0° \leq \phi \leq 60°$ the absorptance is above 99% over the entire frequency range 328 nm $\leq \lambda \leq$ 437 nm. For $\phi = 70°$ the absorptance is above 96%, while for larger angles of incidence the absorptance is lower due to impedance mismatch between air and the silver photonic crystal. We also observe in Figs. 2 and 3 that the absorptance is in general large for $\lambda < \lambda_z$ but decreases substantially at certain incidence angles.

In order to interpret the almost complete absorption in the frequency band 328 nm $\leq \lambda \leq$ 437 nm and in a very wide range of the incidence angle, we calculate the band structure of the corresponding infinite structure. In Fig. 4, we show the band structure of a two-dimensional square lattice of silver cylinders in air with the same lattice parameters a and r_c as in Figs. 2 and 3. In this calculation we neglect absorption by setting the imaginary part of the dielectric constant ϵ_{silver} equal to zero and use experimental data for the real part. (It was found from previous band structure calculations of metallic photonic crystals based on the Drude model that the real part of the band structure is hardly affected by absorp-
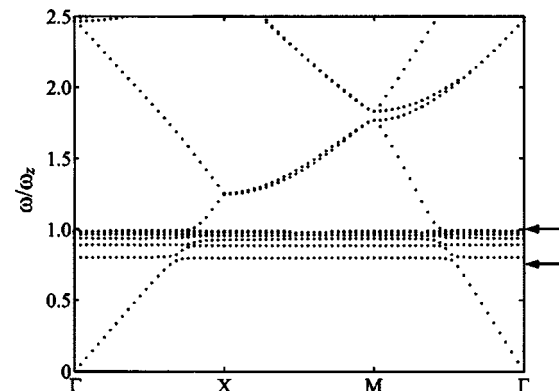

FIG. 4. The calculated band structure of a two-dimensional square lattice of silver cylinders in air. The lattice parameters are the same as in Fig. 2. The arrows indicate the frequency range of intense absorption in Figs. 2 and 3.
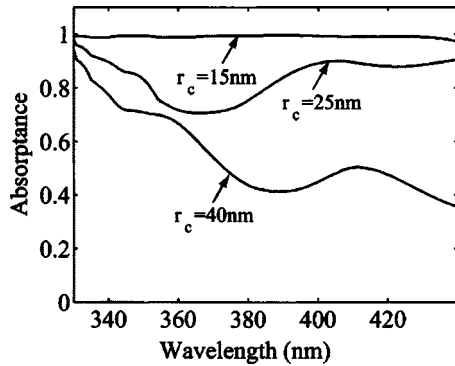
FIG. 5. Absorption spectrum at normal incidence and H polarization for different values of cylinder radius r_c. All other parameters are the same as in Fig. 2.
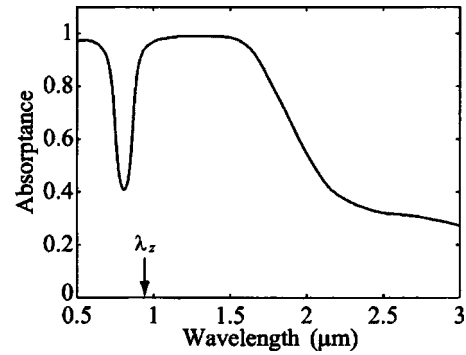

FIG. 6. Absorption spectrum of a finite two-dimensional square lattice of tungsten cylinders in air for normal incidence and H polarization. The lattice parameters are $a=375$ nm, $r_c=55$ nm.

tion for realistic amounts of absorption.[25]) We observe that the band structure consists of a large number of very flat bands in the frequency range of intense absorption. The presence of the flat bands for the H polarization around the surface-plasmon frequency $\omega_{sp}=\omega_p/\sqrt{2}$ is a well-known result of previous calculations based on the Drude model.[25,26,28,29,31] However, as mentioned above, the extent of these bands can only be accurately calculated if experimentally measured data are used for the metallic dielectric constant. The spectrum consists also of a number of air bands that interact with the flat bands in the frequency range of intense absorption. The flat bands have the highest decay rates due to their very small group velocity, and the structure is therefore extremely absorbing in the frequency range of the flat bands.[14,25] Also note that, as these bands extend over all wave vector directions, strong absorption occurs in the photonic crystal for a wide range of incidence angles.

The presence of such flat bands is a necessary but not sufficient condition for creating the strong absorptance. In order for such complete absorption to occur, the photonic crystal must be almost perfectly impedance matched with air over a wide angular and spectral range. Such impedance matching is achieved by adjusting the radius of the cylinders. In Fig. 5, we show the absorptance at normal incidence in the frequency band 328 nm $\leq \lambda \leq$ 437 nm for different values of the cylinder radius r_c. We observe that, as r_c increases, the absorptance decreases substantially. This is due to increased reflection at the interface between air and the photonic crystal, and is expected since, as the metallic volume fraction increases, the crystal approaches an opaque metal slab. For $r_c=15$ nm the absorptance is above 99% and the reflectance below 1%, as mentioned above. For smaller values of r_c we found that, as expected, the reflectance remains below 1%, but the decay length of the incident light inside the photonic crystal increases.

We also found that the reflectance of the structure increases substantially around the Bragg wavelength $\lambda_{Bragg}=2a$ due to Bragg scattering. This causes the dip in absorptance at that frequency observed in Fig. 2. Therefore, to get a wide high-absorption band, the lattice constant a of the crystal has to be either $a<164$ nm or $a>219$ nm so that λ_{Bragg} falls outside the high absorption band 328 nm $\leq \lambda \leq$ 437 nm.

We verified that, if this condition is satisfied, the silver structures exhibit almost complete wide-angle absorption in the spectral range 328 nm $\leq \lambda \leq$ 437 nm.

Similar strong absorption frequency bands are observed in photonic crystals consisting of other metallic materials. As an example, the first zero crossing of the real part of the dielectric constant of tungsten[24] occurs at a wavelength of $\lambda_z \simeq 934$ nm so that the high absorption band of a tungsten photonic crystal structure, similar to the one examined above, is expected to be in the near infrared. In Fig. 6, we show the absorptance for normal incidence and H polarization of a tungsten photonic crystal with lattice parameters $a=375$ nm, $r_c=55$ nm. We indeed observe absorption exceeding 98% in the spectral range 934 nm $\leq \lambda \leq$ 1641 nm. We also observe a dip in absorptance at the Bragg wavelength, as in the silver case.

The almost complete absorption does not appear in the E polarization due to the absence of the flat bands related to surface plasmon polaritons.[25,27,28] However, such flat bands appear in the band structure of three-dimensional metallic photonic crystals.[14,32] Thus, we expect that wide angle almost complete absorption will also be observed in such three-dimensional structures, if the crystal parameters are chosen based on the discussion above.

Finally, we note that the origin of the flat bands are the surface-plasmon resonances of an isolated metallic cylinder.[25,29,33] These resonances occur at discrete frequencies and are strongly localized near the cylinder surface.[25,29] As individual metallic cylinders are brought together to form a photonic-crystal lattice, the discrete resonances broaden into narrow bands.[25,33] The surface-plasmon resonances of an isolated metallic cylinder occur only in the case of H polarization. This explains the absence of flat bands in the band structure of E polarization.[33] Similarly, an isolated metallic sphere exhibits a number of surface-plasmon resonances at discrete frequencies which broaden into narrow bands in a three-dimensional metallic photonic crystal.[14] We also note that the surface-plasmon resonances of isolated small metallic particles are due to the negative real part of the dielectric constant of metals. The exact condition for such a resonance to occur depends on the material properties, and the particle shape. As an example, an isolated small metallic cylinder exhibits a surface-plasmon resonance for ω

$= \omega_p/\sqrt{2}$, or equivalently $\epsilon_{\mathrm{metal}} = -\epsilon_0$, if a lossless Drude model is used.[28] Many metallic materials satisfy such a condition at optical frequencies.[34] The surface-plasmon resonances of metallic cylinders may occur in the visible, ultraviolet, or near infrared, depending on the metallic material.

IV. SUMMARY AND DISCUSSION

In summary, we used the finite-difference frequency-domain method to calculate the absorption spectrum of photonic crystals consisting of metallic cylinders. We first showed that accurate characterization of these structures requires use of experimental data for the frequency-dependent dielectric constant of metals and that the commonly used Drude model results in substantial errors in the calculated absorptance. We found that photonic crystals consisting of metallic cylinders exhibit almost complete wide-angle absorption over a wide spectral range. Strong absorption appears in the *H* polarization due to the presence of a large number of flat bands interacting with air bands. The presence of such flat bands is a necessary but not sufficient condition for creating the almost complete absorptance. The lattice parameters of the crystal must satisfy two additional conditions. First, the metallic volume fraction of the structure must be adjusted through the radius of the cylinders so that the photonic crystal is almost perfectly impedance matched with air. Second, the lattice constant *a* of the crystal has to be chosen so that the Bragg wavelength falls outside the spectral range of the high-decay flat bands. The frequency band of intense absorption is in the visible, ultraviolet, or near infrared, depending on the metallic material.

ACKNOWLEDGMENTS

[1] O. Stenzel, A. Stendal, K. Voigtsberger, and C. von Borczyskowski, Sol. Energy Mater. Sol. Cells **37**, 337 (1995).
[2] M. Westphalen, U. Kreibig, J. Rostalski, H. Luth, and D. Meissner, Sol. Energy Mater. Sol. Cells **61**, 97 (2000).
[3] S. Y. Lin, J. Moreno, and J. G. Fleming, Appl. Phys. Lett. **83**, 380 (2003).
[4] S. Y. Lin, J. G. Fleming, Z. Y. Li, I. El-Kady, R. Biswas, and K. M. Ho, J. Opt. Soc. Am. B **20**, 1538 (2003).
[5] A. K. Sharma, S. H. Zaidi, P. C. Logofatu, and S. R. J. Brueck, IEEE J. Quantum Electron. **38**, 1651 (2002).
[6] H. Huang, Y. Huang, X. Wang, Q. Wang, and X. Ren, IEEE Photonics Technol. Lett. **16**, 245 (2004).
[7] M. Scalora, M. J. Bloemer, A. S. Pethel, J. P. Dowling, C. M. Bowden, and A. S. Manka, J. Appl. Phys. **83**, 2377 (1998).
[8] M. J. Bloemer and M. Scalora, Appl. Phys. Lett. **72**, 1676 (1998).
[9] A. J. Ward, J. B. Pendry, and W. J. Stewart, J. Phys.: Condens. Matter **7**, 2217 (1995).
[10] J. Yu, Y. Shen, X. Liu, R. Fu, J. Zi, and Z. Zhu, J. Phys.: Condens. Matter **16**, L51 (2004).
[11] R. C. McPhedran, N. A. Nicorovici, L. C. Botten, C. M. de Sterke, P. A. Robinson, and A. A. Asatryan, Opt. Commun. **168**, 47 (1999).
[12] Z. Wang, C. T. Chan, W. Zhang, N. Ming, and P. Sheng, Phys. Rev. B **64**, 113108 (2001).
[13] L. C. Botten, N. A. Nicorovici, R. C. McPhedran, C. M. de Sterke, and A. A. Asatryan, Phys. Rev. E **64**, 046603 (2001).
[14] J. B. Pendry, J. Mod. Opt. **41**, 209 (1994).
[15] V. Yannopapas, A. Modinos, and N. Stefanou, Phys. Rev. B **60**, 5359 (1999).
[16] I. El-Kady, M. M. Sigalas, R. Biswas, K. M. Ho, and C. M. Soukoulis, Phys. Rev. B **62**, 15299 (2000).
[17] M. U. Pralle *et al.*, Appl. Phys. Lett. **81**, 4685 (2002).
[18] S. D. Wu and E. N. Glytsis, J. Opt. Soc. Am. A **19**, 2018 (2002).
[19] G. Veronis, R. W. Dutton, and S. Fan, Opt. Lett. **29**, 2288 (2004).
[20] C. P. Yu and H. C. Chang, Opt. Express **12**, 1397 (2004).
[21] S. Guo, F. Wu, S. Albin, and R. S. Rogowski, Opt. Express **12**, 1741 (2004).
[22] J. Jin, *The Finite Element Method in Electromagnetics* (Wiley, New York, 2002), p. 375.
[23] S. Fan, P. R. Villeneuve, and J. D. Joannopoulos, Phys. Rev. B **54**, 11245 (1996).
[24] *Handbook of Optical Constants of Solids*, edited by E. D. Palik (Academic, New York, 1985).
[25] H. van der Lem, A. Tip, and A. Moroz, J. Opt. Soc. Am. B **20**, 1334 (2003).
[26] V. Kuzmiak and A. A. Maradudin, Phys. Rev. B **55**, 7427 (1997).
[27] K. Sakoda, N. Kawai, T. Ito, A. Chutinan, S. Noda, T. Mitsuyu, and K. Hirao, Phys. Rev. B **64**, 045116 (2001).
[28] T. Ito and K. Sakoda, Phys. Rev. B **64**, 045117 (2001).
[29] E. Moreno, D. Erni, and C. Hafner, Phys. Rev. B **65**, 155120 (2002).
[30] M. J. Keskinen, P. Loschialpo, D. Forester, and J. Schelleng, J. Appl. Phys. **88**, 5785 (2000).
[31] H. van der Lem and A. Moroz, J. Opt. A, Pure Appl. Opt. **2**, 395 (2000).
[32] W. Y. Zhang, Z. L. Wang, A. Hu, and N. B. Ming, J. Phys.: Condens. Matter **12**, 5307 (2000).
[33] V. Kuzmiak, A. A. Maradudin, and F. Pincemin, Phys. Rev. B **50**, 16835 (1994).
[34] A. D. Rakic, A. B. Djurisic, J. M. Elazar, and M. L. Majewski, Appl. Opt. **37**, 5271 (1998).